Volume 203, number 1 CHEMICAL PHYSICS LETTERS 12 February 1993

Lifetimes of electronically excited states of molecules on oxide versus metal surfaces

R.M. Jaeger, K. Homann, H. Kuhlenbeck and H.-J. Freund

Physikalische Chemie 1, Ruhr-Universität Bochum, Universitätsstrasse 150, W-4630 Bochum, Germany

Received 9 October 1992; in final form 19 November 1992

The optically forbidden ${}^1\Sigma^+ \rightarrow a\,{}^3\Pi$ transition of CO adsorbed on an epitaxially grown $Al_2O_3(111)$ surface has been studied by means of electron energy loss spectroscopy. On this surface several CO adsorption states exist with adsorption enthalpies ranging from 88 (multilayer) to 170 meV. For the first time even in the (sub)monolayer range the vibrational fine structure of the energy loss peaks due to the ${}^1\Sigma^+ \rightarrow a\,{}^3\Pi$ electronic transition of adsorbed CO could be clearly resolved. The half widths of the loss peaks have been used to estimate the lifetimes of the excited states.

Excited state lifetimes of adsorbed molecules are important for desorption processes involving electronic transitions at surfaces (DIET). Spectroscopies like LID (laser-induced desorption), ESD (electron stimulated desorption), and PSD (photon stimulated desorption) deal with such processes [#1].

Lifetimes of excited states are important parameters for desorption processes because they considerably influence the desorption probabilities [1–4]. The energy of excited adsorbate states on metals can rapidly be dissipated into the solid by low-energy electron–hole pair creation and Auger deexcitation, which is not the case to the same extent for substrates with no electronic density of states at the Fermi edge. This means that lifetimes of excited states of adsorbates are usually considerably shorter on metals than on non-conducting materials and therefore the desorption yields are smaller, as is well known from LID, ESD and PSD experiments [5–7].

Due to its high surface sensitivity EELS (electron energy loss spectroscopy) is well suited to study electronic excitations of adsorbates at surfaces. Especially at low primary electron energies, not only optically allowed but also dipole forbidden transitions like the ${}^1\Sigma^+ \rightarrow a\,{}^3\Pi$ excitation may be observed. Adsorbates on metal surfaces usually exhibit rather broad loss peaks because, as explained before, the excited state lifetime is rather short. Therefore no data for vibrationally resolved electronic transitions of adsorbed CO exist in the literature although these splittings are well resolved in the gas phase and in multilayer CO films. Considerable information on the initial and final state potential is contained in the structure of the vibrational series so that it is highly desirable to get access to the vibrational fine structure also for adsorbates. Only few reports on vibrationally split electronic transitions of adsorbates may be found in the literature. For the case of the low-energy $a\,{}^1\Delta_g$ excitation of molecular oxygen on silver and graphite clear vibrational splittings could be observed [8,9] and, using NEXAFS (near edge X-ray absorption fine structure), the vibrational fine structure of the $C1s \rightarrow \pi^*$ transition of C_2H_4 and C_2D_4 adsorbed on Cu(100) and Ag(100) could be resolved [10].

The situation is different when non-conducting materials like oxides are used as substrates. Especially for aluminium oxide, where the electronic band gap is rather large, long lifetimes have to be expected. For this reason we could resolve the CO $a\,{}^3\Pi$ vibrational splittings even at (sub)monolayer coverages. As revealed by TDS (thermal desorption spectroscopy) several CO species with different ad-

---

[#1] Introductions to the experimental and theoretical aspects of DIET may be found in the proceedings of the DIET workshops; for DIET 1 see ref. [1], for DIET 2 ref. [2], for DIET 3 ref. [3] and for DIET 4 ref. [4].

0009-2614/93/$ 06.00 © 1993 Elsevier Science Publishers B.V. All rights reserved.

sorption energies exist at the surface so that we could study the lifetime broadening as a function of the initial state adsorbate–substrate interaction strength.

The experiments have been performed in a magnetically shielded UHV system designed for angular-resolved ultraviolet photoelectron spectroscopy (ARUPS) and angular-resolved electron energy loss spectroscopy. The electron energy analyzer is mounted on a goniometer allowing for angular-resolved electron detection in two orthogonal planes. For the EELS experiments the overall resolution of analyzer plus electron monochromator was set to 50 meV.

The NiAl(110) single crystal was mounted on a liquid He flow cryostate which allowed for cooling down to about 25 K. Heating was possible by electron impact from a filament mounted behind the back of the crystal. After cleaning the sample using standard sputtering and heating sequences the oxide film was prepared by admitting 1200 L ($1\ \mathrm{L}=10^{-6}$ Torr s) of oxygen at elevated temperature (550 K) with subsequent annealing to T = 1200 K as described elsewhere [9]. The quality of the resulting thin oxide film was checked by LEED. For the final oxide layer a manifold of sharp LEED spots with low background intensity was observed, indicative of a well-ordered oxide structure. Films prepared in this way have a thickness of about 5 Å [9].

To avoid contamination of the CO layer from the residual gas atmosphere during the measurements it was flashed off every 20 min and the surface was prepared anew.

For CO on Ag(110) the coverage was calibrated by the onset of the multilayer desorption signal (T=38 K) in TDS and by the onset of the vibrational splitting of the a $^3\Pi$ loss in EELS. As will be discussed below the vibrational splitting is only observed for coverages above one monolayer. Both methods gave a dose of about 1.2 L for a full monolayer. As concluded from TDS and from the EELS data discussed below, for CO/Al_2O_3/NiAl(110) already at doses somewhat below 1 L second layer adsorption is observed. Whether this points towards a less densely packed first layer or to a different sticking coefficient or to some kind of Vollmer–Weber growth mode cannot, however, be answered from our data.

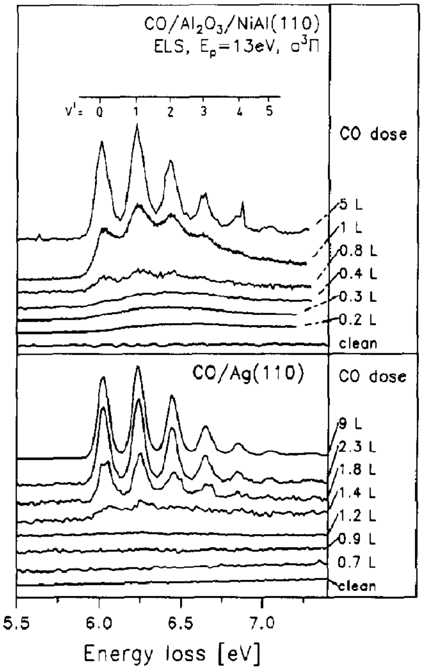

Fig. 1. Comparison of the CO $^1\Sigma^+ \rightarrow$ a $^3\Pi$ energy loss spectra for CO on $Al_2O_3(111)$/NiAl(110) (top) and Ag(110) (bottom) as a function of the CO dose.

In fig. 1 two sets of EEL spectra of the CO $^1\Sigma^+ \rightarrow$ a $^3\Pi$ excitation are shown as a function of the CO coverage for CO/Al_2O_3/NiAl(110) (top) and for CO/Ag(110) (bottom) [10]. The primary electron energy was 13 eV in both cases. As may be visualized from fig. 1 at coverages below a monolayer ($\approx$ 1.2 L for CO/Ag(110) and $\approx$1 L for CO/Al_2O_3(111)/NiAl(110), respectively) more or less no adsorbate signal is observed for the CO adsorbate on the metal, whereas on the oxide surface already at the lowest coverage a well developed loss due to the adsorbate is visible. At multilayer coverages the spectra look similar for the metal and the oxide substrate as expected. The different behaviour in the submonolayer range is, as already discussed, due to differences in the excited state lifetimes. In the submonolayer coverage range the lifetime of the a $^3\Pi$ excited state of CO/Ag(110) is so short that the energy loss features are smeared out over a large energy range and are therefore hardly separable from the background intensity.

The adsorption behaviour of CO on the thin aluminium oxide film is a complicated function of the

CO coverage. As revealed by TDS (see inset of fig. 2) two different CO species exist in the (sub)monolayer coverage range with desorption temperatures of 55 and 67 K. Additional desorption signals are obverved at 38 and 47 K. The first one is attributed to multilayer desorption whereas the second one is most likely due to CO molecules adsorbed in the second layer. These two species could, however, not be differentiated by EELS. The interaction with the substrate is different for these four species and this is also visible in the energy loss spectra. A set of EEL spectra of the $^1\Sigma^+ \rightarrow a\,^3\Pi$ excitation of CO on Al_2O_3 is shown in fig. 2 as a function of the CO coverage. The spectra have been fitted using student functions. For the losses of each Franck–Condon series the fwhms have been chosen to be the same. In accord with the TD data we assumed that dependent on coverage three different CO species with different fwhms and slightly different excitation energies and Franck–Condon envelopes contribute to the loss peaks. The losses in the spectrum taken at lowest coverage (0.2 L) are entirely due to the most strongly bound species with a desorption temperature of about 67 K whereas the losses in the upmost spectrum in fig. 2 are mostly due to the CO bi- and multi-layer. In the other spectra (0.3 L and 1 L) also a third species ($T_{des}=55$ K) contributes with significant intensity. Interestingly the $a\,^3\Pi$ ($v'=0$) excitation of the most strongly bound species species is shifted by about 170 meV to higher energy with respect to the other species. Also, the loss spectra taken at lower coverage show less pronounced vibrational splittings. The fitting parameters for the four species are listed in table 1 in comparison with gas-phase data. Also included in table 1 are the adsorption enthalpies calculated from the TDS data using the Redhead formula [13] and the lifetimes as calculated from the loss halfwidths via the energy–time uncertainty relation $\delta E \delta t \geq \hbar$. For the half widths given in table 1 it has been assumed that the analyzer and monochromator transmission functions can be represented by Gaussians. Under this assumption the fwhm of the elastically scattered beam has been deconvoluted from the fwhms of the loss features.

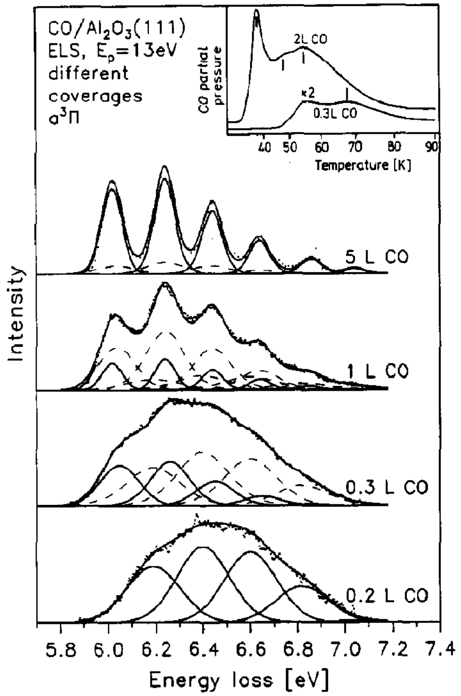

Fig. 2. Fits of energy loss spectra of CO on Al_2O_3(111)/NiAl(110) for different CO coverages. In the inset thermal desorption spectra for two different CO doses are shown.

The lifetimes of the $a\,^3\Pi$ excited states given in table 1 must be considered as lower bounds to the real lifetime because the loss features may additionally be broadened by other effects. These effects are (i) excitation of substrate phonons and adsorbate–substrate vibrations during the primary excitation process according to the Franck–Condon principle and (ii) a thermal spread of energies in the initial state.

The mechanism of process(i) is shown in fig. 3. The energy needed to excite a CO molecule from the $^1\Sigma^+$ ground state to a certain vibrational level of the $a\,^3\Pi$ state is the energy difference between these two states. When the molecule is adsorbed on a surface the energy of the initial state as well as that of the final state may shift, leading to a different excitation energy (left part of fig. 3). This could be the reason for the shift of the excitation energies of the (sub)monolayer CO species. However, this simple picture is incomplete because the interaction with the substrate not only shifts the initial and final state energies of the CO molecules but also allows, according to the Franck–Condon principle, for participant excitation of vibrations like the different molecule–substrate vibrations and substrate phonons. For the case of vibration of the molecule parallel to

Table 1
Parameters of the three different CO species on $Al_2O_3(111)$/NiAl(110) in comparison with gas-phase data. For the (sub)monolayer species the adsorption enthalpy has been calculated from TDS data via the Redhead formula [13] whereas for the multilayer it has been taken from ref. [14]. The other parameters have been derived from the fits shown in fig. 2. Gas-phase parameters have been taken from ref. [15]

Species	Adsorption enthalpy (meV)	fwhm (meV)	$E(v'=0)$ (eV)	$E(v'=1)-E(v'=0)$ (meV)	Lifetime (10^{-15} s)
$T_{des}=67$ K	−170	260±7	6.19±5	210±7	2.5
$T_{des}=55$ K	−140	190±7	6.04±5	200±7	3.5
multilayer	−88	70±7	6.02±5	200±7	9.4
gas phase			6.02	202	some ms

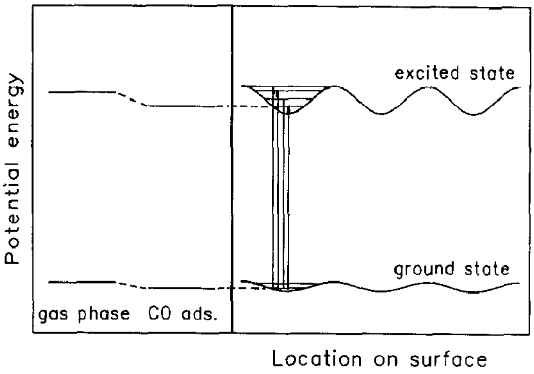

Fig. 3. Potential energy diagrams for gas-phase CO and adsorbed CO. For details see text.

the surface this is schematically depicted in the right part of fig. 3. The adsorbate–substrate potential will be corrugated according to the periodicity of the substrate with the corrugation amplitudes likely being different for the initial and the final state [16]. The well-defined levels of the gas-phase molecules now split due to the different levels of vibration parallel to the surface, which is of course an additional source of broadening and peak shift. In this manner also the other molecule–substrate vibrations and the substrate phonons contribute to the form and the energy positions of the losses.

To estimate the contribution of vibrational broadening we referred to optical excitation spectra for CO isolated in rare-gas matrices. This can be done because the electronic structure of the O^{2-} ions, which most likely build up the topmost layer of the Al_2O_3 substrate, is similar to that of neon. Thus the halfwidths of the $^1\Sigma^+ \rightarrow a\,^3\Pi$ optical absorptions in the rare gas matrix may serve as an estimate for the contributions of (i) to the halfwidths of the energy loss peaks. According to Bahrdt et al. [17,18] this contribution is about 24 meV, independent of the rare-gas matrix.

The contribution of (ii) to the overall fwhm will be rather small. Assuming an average thermal energy of $\frac{1}{2}kT$ per degree of freedom this amounts to about 8 meV at $T=30$ K. Thus the contribution of (i) and (ii) to the experimentally determined halfwidth will only be about 32 meV. Since this value is rather small compared to the numbers given in table 1, at least for the (sub)monolayer species, the real lifetimes will not greatly from the ones given in table 1.

Another contribution to the broadening could be of electronic nature. If the CO molecules lie flat on the surface then the $2\pi^*$ levels may be split due to different interactions with the substrate. The amount of additional broadening is not known. However, since the molecules are only physisorbed, which means that the surface-molecule distance may be about 4 Å, this effect is expected to be small.

Finally we would like to comment on the results presented in table 1. The observed lifetimes are rather large compared to the time electronic excitations need to occur, which is about 10^{-16} s. The reason is that the energy of the $a\,^3\Pi$ excited state is not sufficient to excite electron–hole pairs in the substrate, which takes at least 9.5 eV. Thus the excited CO state cannot deexcitate by electron–hole pair creation in the aluminium oxide substrate. Auger deexcitation is also strongly hindered: an intramolecular Auger process is not possible because the $a\,^3\Pi$ state is the lowest excited state of the CO molecule and an Auger process involving the substrate electrons is also impossible since the ionization energy of the highest occupied substrate level is about 5 eV with respect to the Fermi energy, which means that it needs 9.3 eV (Φ=4.3 eV) to take an electron out of the substrate [8]. This is too much for the a $^3\Pi$ excited state. It should however be considered that the Auger final state is positively charged. Due to the close proximity of the molecule to the negatively charged oxygen ions of the first substrate layer the Auger final state may be stabilized by several electron volts and Auger processes may become possible. The estimated lifetimes are in principle consistent with Auger deexcitation processes because such processes usually need some 10^{-15} s to occur. However, whether Auger processes are possible or not, only a limited number of deexcitation channels exist for the a $^3\Pi$ excited CO molecules and comparably high lifetimes result. From this discussion it should be clear that the situation is different on metal substrates. Here neither electron–hole pair creation in the substrate nor Auger deexcitation involving a substrate electron are considerably hindered so that the CO a $^3\Pi$ lifetime on metals will be much shorter. Therefore for all studied CO adsorbates including CO/Ag(110) only a rather broad structure is observed instead of a vibrationally resolved series of transitions.

We thank the Deutsche Forschungsgemeinschaft (DFG) and the Ministerium für Wissenschaft und Forschung des Landes Nordrhein-Westfalen for funding our research. HJF gratefully acknowledges financial support by the Fonds der Chemischen Industrie.

References

[1] N.H. Tolk, M.M. Traum, J.C. Tully and T.E. Madey, eds., Springer series in surface science, Vol. 4 (Springer, Berlin, 1983).

[2] W. Brenig and D. Menzel, eds., Springer series in surface science, Vol. 13 (Springer, Berlin, 1985).

[3] R.H. Stulen and M.L. Knotek, eds., Springer in surface science, Vol. 19 (Springer, Berlin, 1988).

[4] G. Betz and P. Varga, eds., Springer series in surface science, Vol. 24 (Springer, Berlin, 1990).

[5] D. Menzel, Topics in applied physics, Vol. 4. Interaction on metal surfaces, ed. R. Gomer (Springer, Berlin, 1975).

[6] M. Menges, B. Baumeister, K. Al-Shamery, B. Adam, T. Mull, H.-J. Freund, C. Fischer, D. Weide and P. Andresen, Springer series in surface science, DIET 5, submitted for publication.

[7] Th. Mull, B. Baumeister, M. Menges, H.-J. Freund, D. Weide, C. Fischer and P. Andresen, J. Chem. Phys. 96 (1992) 7108.

[8] D. Schmeisser, J.E. Demuth and P. Avouris, Phys. Rev. B 26 (1982) 4857.

[9] E.T. Jensen and R.E. Palmer, Surface Sci. 237 (1990) 153.

[10] H. Rabus, D. Arvanitis, M. Domke and K. Baberschke, J. Chem. Phys. 96 (1992) 1560.

[11] R.M. Jaeger, H. Kuhlenbeck, H.-J. Freund, M. Wuttig, W. Hoffmann, R. Franchy and H. Ibach, Surface Sci. 259 (1991) 235.

[12] K. Homann, R.M. Jaeger and H. Kuhlenbeck, J. Electron Spectry., submitted for publication.

[13] P.A. Redhead, Vacuum 12 (1962) 203.

[14] Gmelins Handbuch der anorganischen Chemie, Part C(1) (Verlag Chemie, Weinheim, 1970) p. 183.

[15] N. Swanson, C.E. Kuyatt, J.W. Cooper and M. Krauss, Phys. Rev. Letters 28 (1972) 948.

[16] N. Mårtensson and A. Nilsson, J. Electron Spectry. 52 (1990) 1.

[17] J. Bahrdt, P. Gürtler and N. Schwentner, J. Chem. Phys. 86 (1987) 6108.

[18] J. Bahrdt and N. Schwentner, J. Chem. Phys. 88 (1988) 2869.